

# Polarimetry of powerful radio galaxies from $z = 0$ to $z = 4$

Clive Tadhunter

*Department of Physics & Astronomy, University of Sheffield, Sheffield  
S3 7RH, UK*

**Abstract.** The advent of sensitive polarimeters on large telescopes has led to a revolution in our understanding of active galaxies over the last 20 years. In the case of powerful radio galaxies the deep polarimetric measurements made possible by the new technology have: (a) provided the most direct evidence to support the unified schemes for powerful radio galaxies; (b) enhanced our understanding of the colours and morphologies of radio source host galaxies at all redshifts; and (c) provided key information about the kinematics and geometries of the scattering regions on a sub-kpc scale.

## 1. Introduction

Active galactic nuclei (AGN) are luminous, radiate their continuum light anisotropically, and are embedded in a rich ISM that contains plentiful scattering particles such as electrons and dust grains. It is not surprising, therefore, that polarimetric studies of the scattered light component provide a key tool for investigating the geometry, kinematics and host galaxy properties of active galaxies. In this review I will concentrate on polarimetry of powerful radio galaxies, which form a well-defined class of active galaxies, selected on the basis of their extended radio emission. Apart from clean selection criteria, radio galaxies have the additional advantage that the directions of their radio jets provide useful geometrical information.

Polarimetry is a “photon hungry” subject, but radio galaxies are relatively faint and distant. Therefore the detailed polarimetric study of powerful radio galaxies at optical wavelengths only began in earnest in the early 1980s when polarimeters began to be used with sensitive electronic detectors on large telescopes.

The pioneering work was done by Antonucci (1982, 1984) who reported spectropolarimetric observations of 31 nearby 3C radio galaxies ( $z < 0.26$ ) made with the IDS on the Lick telescope. Although his survey was limited in its sensitivity, Antonucci’s results prefigure much of the modern polarimetric study of radio galaxies. For example, Antonucci was the first to deduce that most of the optical polarization properties of nearby radio galaxies can be explained in terms of scattered AGN light, with the variety in the alignments of the polarization E-vectors accounted for by different configurations of the scattering medium. Antonucci was also the first to propose the presence of an optically thick central obscuring region in radio galaxies, requiring scattering at the poles of a torus structure to explain the perpendicular alignments of the optical polarization vectors relative to the radio axes in some objects.

Following Antonucci's early work, the use of sensitive CCD-based waveplate polarimeters on 4m telescopes in the late 1980s allowed accurate imaging polarimetry measurements to be made of more distant radio galaxies out to a redshift of  $z \sim 1$ . Then, the subsequent introduction of 8m class telescopes both further extended the redshift range available for polarimetric investigations of distant radio galaxies (up to  $z \sim 4$ ), and also facilitated deeper spectropolarimetric studies of nearby sources. Finally, since 1994 the polarimeters on the post-COSTAR HST have allowed high spatial resolution imaging polarimetry observations to be made of the inner structures on a sub-kpc scale at both optical and dust-penetrating near-IR wavelengths.

In the following I will demonstrate that the high sensitivity polarization measurements of the scattered light component allowed by these technological innovations have led to major advances in several key areas of radio galaxies research. A full list of references for optical/UV polarization studies of the scattered light in powerful radio galaxies is presented in the Table 1 of the Appendix.

## 2. Polarimetric tests of the unified schemes

The unified schemes for powerful radio sources provide a useful framework for understanding the relationships between the various sub-classes of radio loud AGN. In the strongest versions of such schemes it is proposed that radio galaxies and radio-loud quasars are the same thing viewed from different directions, with the quasar light blocked off from our direct view in the radio galaxies by central obscuring tori (e.g. Barthel 1989). Until the early 1990s attempts to test such schemes were indirect and involved the statistical comparisons between the radio and optical properties of samples of radio galaxies and radio-loud quasars (e.g. Barthel 1989, Jackson & Browne 1990). However, such statistical comparisons are not capable of providing a true test by determining whether or not *individual* radio galaxies contain quasar nuclei hidden in their cores.

Polarimetric observations have the potential to provide a more direct test of the unified schemes. If the quasar is luminous enough and there is sufficient scattering ISM in the quasar illumination cones, a measurable amount of the optical/UV light of the hidden quasar nucleus will be scattered into our line of sight. The scattered component will be highly polarized. Thus measurements in polarized light enhance the contrast of the scattered component relative to the (unpolarized) direct emission from the stars and gas in the host galaxies. In this way it is possible to detect the scattered quasar emission polarimetrically, even if it is not readily apparent in the straight intensity images and spectra.

In fact, the first polarimetric detection of this scattered quasar component came well before the unified schemes gained prominence: in his pioneering work Antonucci (1984) detected a broad quasar-like  $H\alpha$  line in the polarized intensity spectrum of the N-galaxy 3C234.

The detailed study of the scattered quasar component had to await the introduction of sensitive CCD-based waveplate polarimeters. First, imaging polarimetry observations using 4m class telescopes demonstrated that the nuclei of some low redshift radio galaxies are surrounded by spatially resolved optical reflection nebulae, with the polarization E-vectors aligned perpendicular to the

radius vectors from the nuclei, as expected for scattered nuclear light. Examples include PKS2152-69 (di Serego Alighieri et al. 1988) and Cygnus A (Tadhunter et al. 1990). Subsequently, several more reflection nebulae were detected in radio galaxies across a wide range of redshift (e.g. Tadhunter et al. 1992, Cimatti et al. 1993, Draper et al. 1993). Most recently, deep spectropolarimetry observations with 8m telescopes have detected the broad permitted lines (e.g.  $H\alpha$ , MgII) characteristic of scattered quasars in the polarized intensity spectra of nearby radio galaxies (Ogle et al. 1997, Cohen et al. 1999). These latter observations represent the best, most direct evidence that at least *some* powerful radio galaxies contain luminous hidden quasar nuclei.

However, several factors can make the scattered quasar component difficult to detect. These include (depending on the object): a lack of a sufficient scattering medium; relatively low luminosity quasar nuclei; dilution by unpolarized starlight of the host galaxy; dilution by unpolarized AGN-related components (see below); and the geometrical dilution caused by integrating the polarization vectors across the broad illumination cones. Therefore, it is doubtful that polarimetric observations ever will provide an answer to the question of whether *all* radio galaxies contain hidden quasar nuclei, as suggested by the strongest versions of the unified schemes.

### 3. The UV excess in powerful radio galaxies: starbursts or AGN pollution?

One of the major motivations for studying powerful radio galaxies is that they represent potentially important probes of the evolution of giant elliptical galaxies in the high redshift universe. However, if we are to use radio galaxies in this way it is essential to understand their continuum spectral energy distributions (SEDs). In particular, it is crucial to distinguish the continuum components that are specifically related to the star formation in the host galaxies, from those that are a direct consequence the AGN activity.

In the early 1980s photometric studies of the optical-infrared colours of the radio galaxies at  $z > 0.5$  demonstrated that such objects show significant UV excesses compared with normal, passively-evolving early-type galaxies (e.g. Lilly & Longair 1984). At the same time imaging studies revealed that the excess UV light is distributed in elongated, multi-modal structures that are quite unlike those of elliptical galaxies in the low redshift universe (Lilly, Longair & McClean 1983). Both the colours and UV structures of the high- $z$  radio galaxies were initially interpreted in terms of starbursts associated with the evolution of the host galaxies. However, with the discovery that the UV structures are closely aligned with the axes of the large-scale radio structures – the so-called “alignment effect” (McCarthy et al. 1987, Chambers et al. 1988) – it became clear that the extended UV emission might be related more to the effects of the activity than the evolution of the host galaxies. Indeed, it was proposed that aligned UV structures represent the giant reflection nebulae illuminated by the hidden quasar nuclei (Tadhunter et al. 1988, Fabian 1989). In this case the UV light should be highly polarized.

The first attempts to test the reflection nebula idea using CCD-based polarimeters on 4m telescopes proved successful (di Serego Alighieri et al. 1989,

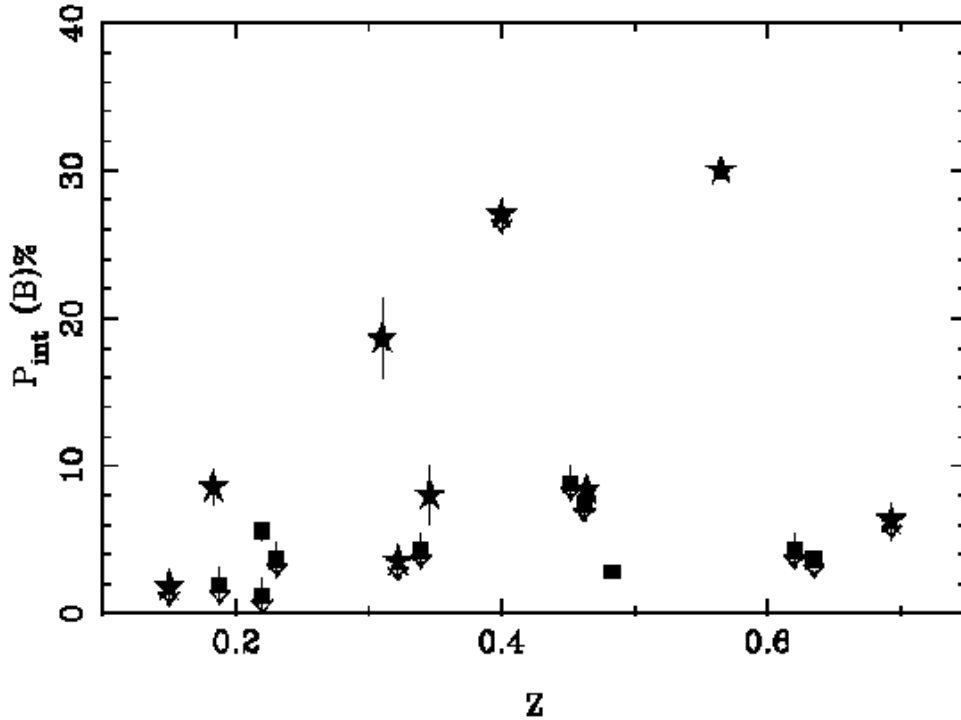


Figure 1. B-band polarization plotted as a function of redshift for the 2Jy sample (see Tadhunter et al. 2002 for details). The measured polarization values have been corrected for the dilution by the light of the old stellar populations and the nebular continuum. They have also been corrected for Ricean bias. Stars indicate narrow line radio galaxies, whereas squares indicate broad line radio galaxies. Upper limits are indicated by arrow symbols.

Januzzi & Elston 1991, Tadhunter et al. 1992). High degrees of linear polarization were detected in the UV continua of several high redshift radio galaxies. Moreover, the polarization E-vectors were found to be aligned perpendicular to axes of the large-scale radio and UV structures, as expected for anisotropic illumination by a central point source. With the advent of 8m telescopes it became possible to map the polarization of the high-z objects in detail, perform spectropolarimetry, and extend the polarimetric studies out to higher redshifts (see Table 1 for a full list of references). The main general conclusions of these studies are as follows.

- **Incidence of scattered UV emission.** The extended UV emission is dominated by scattered quasar light in some, but not all, high redshift radio galaxies.
- **Scales of the refelection nebulae.** The reflection nebulae can be galaxy scale, extending 10s of kpc from the nuclei of the host galaxies in some objects.

- **Nature of the scattering medium.** The dominant scattering particles are likely to be dust grains; the Thompson depth for electron scattering is insufficient to produce the luminosity of the scattered light in most objects.
- **Distribution of scattering particles.** The scattering is approximately grey, and the scattering dust is likely to be distributed in small optically thick clouds (Vernet et al. 2001, Kishimoto et al. 2001).

Although these results help to explain the alignment effect in high redshift radio galaxies, and lend strong support to the orientation-based unified schemes (see above), they also suggest that much of the UV emission in these objects represents “AGN pollution”.

This raises the issue of the extent to which the scattered quasar light dominates the excess UV emission in the general population of powerful radio galaxies. Accurate polarimetric observations of distant radio galaxies are challenging. Therefore, the early studies were biased towards the brightest, most spectacular objects in any redshift range and do not necessarily provide an accurate indication of the importance of the scattered quasar component. In order to avoid this selection effect we have carried out a combined spectroscopic and imaging polarimetric survey of a complete, optically unbiased sample of 19 southern 2Jy radio galaxies with redshifts in the range  $0.15 < z < 0.7$  (Tadhunter et al. 2002). All of the objects in this sample show evidence for UV continuum excesses, and by making the polarimetric observations in the B-band we have sampled the rest-frame UV in all the objects in the sample. The results are shown in Figure 1, where the polarization measurements have been corrected for dilution by the light of the old stellar populations in the host galaxies and nebular continuum. Taking into account the geometrical dilution caused by integrating the polarization over the broad quasar illumination cones, we would expect to measure polarization at the  $>10\%$  level if the UV excess is dominated by scattered light (Manzini & di Serego Alighieri 1996). While a few objects in our sample are polarized at such a high level, most objects are polarized at a lower level, suggesting that their excess UV emission is not dominated by scattered quasar light.

What other components might contribute to the UV excess? Careful modelling of the polarimetric results in combination with the emission line and continuum spectra for the 2Jy sample has revealed a complex picture. In fact, we find that the following four components contribute to the UV excess to varying degrees.

- **Scattered quasar light.** This is detected in 32% of objects, and dominates in  $\sim 15\%$  of objects.
- **Nebular continuum.** This is significant in all objects with strong emission lines, contributing 3 - 40% of the excess UV emission (see Dickson et al. 1995).
- **Direct AGN light.** The unpolarized continua of low-luminosity, or partially obscured, broad line nuclei make a substantial contribution to the UV excess in 40% of the objects in our sample.

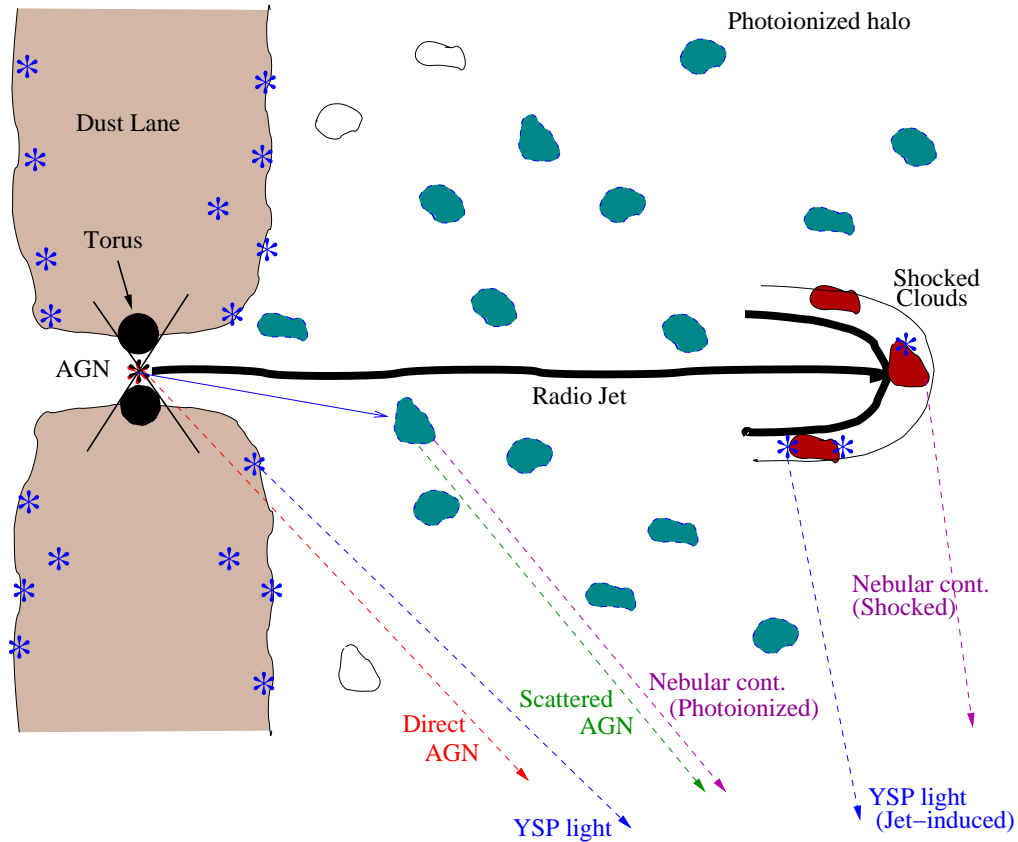


Figure 2. Components contributing to the UV excess in powerful radio galaxies. Components include: scattered AGN light, nebular continuum from the warm emission line gas (both shocked and photoionized), direct AGN light from partially obscured AGN, and the light of the young stellar populations (YSP) in the host galaxies.

- **The light of young stellar populations (YSP).** This makes a significant contribution to the UV excess in 30 - 50% of the objects in our sample.

Figure 2 illustrates the various components that contribute to the UV excess. The complexity revealed by our polarimetric/spectroscopic survey of the 2Jy sample is also apparent in high resolution HST images of powerful radio galaxies such as Cygnus A (Jackson, Tadhunter & Sparks 1998). However, in spite of the complexity, our results demonstrate that it is possible to detect the young stellar populations and investigate the evolution of host galaxies, provided that high quality spectroscopic and polarimetric data are available.

An important lesson from these studies is that it is dangerous to interpret the colours and SEDs of distant active galaxies solely in terms of the properties of the stellar populations in the host galaxies without first quantifying the degree of AGN pollution.

#### 4. Investigating the structures and kinematics on a sub-kpc scale

Recently, attention has turned to using polarimetric observations to investigate the structures and kinematics on the sub-kpc scale — an important scale for investigating the impact of the activity on the host galaxies, as well as the structure of the emitting regions in the immediate vicinity of the super-massive black holes. The contributions by J. Smith and M. Kishimoto at this conference demonstrate the potential of spectropolarimetric observations for studying the BLR and inner accretion disks of active galaxies (see Smith et al. 2004, Kishimoto et al. 2003). I will give two further examples of the use of polarimetry as a tool for probing the central regions of radio-loud active galaxies.

##### 4.1. Near-IR polarimetry observations of Cygnus A

Near-IR observations can provide further tests of the unified schemes and allow investigations of the radiation field anisotropy and continuum emission mechanisms at longer wavelengths than the optical observations described above. The near-IR observations also have the advantage that, since they are less sensitive to dust obscuration, they have the potential to probe regions closer to the central AGN.

Some powerful radio galaxies have near-IR core sources that are unresolved in ground-based observations (e.g. Simpson et al. 1995). Although these compact core sources have been interpreted in terms of the quasar light “shining through” the torus at less heavily obscured near-IR wavelengths, the extinctions deduced from the near-IR colours and fluxes are significantly lower than the those deduced from X-ray measurements of the absorbing columns (see Tadhunter et al. 1999).

In order to investigate the true nature of the compact near-IR core sources we have used the capabilities of NICMOS on the HST to make high spatial resolution imaging polarimetry observations of the archetypal radio galaxy Cygnus A at  $2.0\mu\text{m}$  (Tadhunter et al. 1999, 2000). The results are shown in Figure 3. The intensity images reveal a compact core source that is unresolved at the  $<0.2$  arcsec resolution of the observations, but this core source is highly polarized at the  $>28\%$  level, with the polarization E-vector aligned perpendicular to the radio axis. It is difficult to reconcile the near-IR colours and fluxes with the large extinction required to produce the polarization by dichroic extinction. Therefore it is likely that the core source does not represent transmitted quasar light, but rather quasar light scattered by the far wall of the torus or by a polar scattering region. This helps to explain the discrepancy between near-IR and X-ray based estimates for the torus extinction in this source.

The near-IR imaging observations also reveal an extended, edge-brightened bi-cone structure that is likely to be due to a combination of scattered quasar light and redshifted  $\text{Pa}\alpha$  emission. In contrast to the optical polarization map (Ogle et al. 1997), the optical emission line cones (Jackson et al. 1998), and the near-IR  $2.0\mu\text{m}$  intensity image (Figure 3), which all show reflectional symmetry about the radio axis, the near-IR polarization is concentrated along the NW-SE wall of the bicone. This suggests that, while the short wavelength X-ray to optical radiation is isotropic within the cones defined by the torus, the near-IR radiation is *intrinsically anisotropic* within the cones. The most plausible ex-

planation for such intrinsic anisotropy is that the near-IR continuum associated with the AGN is emitted by the warped outer part of the accretion disk; the NW-SE wall sees a larger surface area of the near-IR emitting region than the SW-NE wall. Indeed, such warping is predicted by models for radiation induced instabilities in accretion disks (e.g. Pringle 1997).

These observations of Cygnus A demonstrate the potential of high resolution near-IR polarimetry observations for investigating the radiation field anisotropy in structures ranging from the sub-pc scale outer accretion disk surrounding the central AGN, to the kpc-scale reflection nebula associated with the dust lane.

#### 4.2. Scattering outflows in the NLR of Cygnus A

A further interesting feature of the near-IR intensity images of Cygnus A is that they reveal the cones to be hollowed out close to the nucleus (see Figure 3, top left), presumably as a consequence of outflows driven by the powerful AGN activity (Tadhunter et al. 1999). The question then arises as to whether there is any kinematic evidence for the outflows that are hollowing out the cones.

Outflows are notoriously difficult to detect in the extended regions of distant active galaxies, because of uncertainties about the true systemic velocities of the host galaxies, and the likely combination of gravitational (inflow, rotational) and AGN-induced (outflow) motions. As part of a detailed study of Cygnus A designed to measure the mass of the central black hole, we have used the [OIII] $\lambda$ 5007 line to map the emission line kinematics close to the AGN at 0.1 arcsec (0.1 kpc) resolution using STIS/HST (Tadhunter et al. 2003). The steep velocity gradient across the nucleus revealed by these observations is consistent with rotational motion about a  $(2.5 \pm 0.5) \times 10^9 M_{\odot}$  black hole. However, we also detect a component 0.2 arcsec from the nucleus in the centre of the cone that is redshifted by  $\sim 400 \text{ km s}^{-1}$  relative to the rest frame of the host galaxy. This component cannot be reconciled with rotational motion associated with either the central disk or the kpc-scale dust lane. It is also difficult to explain the redshift of this component in terms of direct [OIII] emission from the AGN-induced outflow, since the NW cone is tilted towards our line of sight.

Clues to the nature of the strongly redshifted component are provided by the spectropolarimetry observations reported by van Bemmelen at this conference (see also van Bemmelen et al. 2003). In an aperture that encompasses the entire nuclear region of Cygnus A, van Bemmelen et al. detect an [OIII] feature in the polarized intensity spectrum that is redshifted by the same amount ( $\sim 350 - 450 \text{ km s}^{-1}$ ) as the redshifted component detected along the radio axis in our STIS/HST data. Therefore it is likely that this latter component represents [OIII] emission from an inner narrow line region that has been scattered by outflowing dust in the NW cone. Since a scattering outflow will always produce a redshifted feature, this explanation avoids the geometrical problem of attempting to explain the redshifted feature in terms of direct [OIII] emission from an outflow in the NW cone.

Clearly, deep spectropolarimetry observations of the narrow line emission provide a useful tool for investigating the significance of activity-induced outflows in powerful radio galaxies. It will be important to extend such observations to larger samples of radio galaxies in the future.



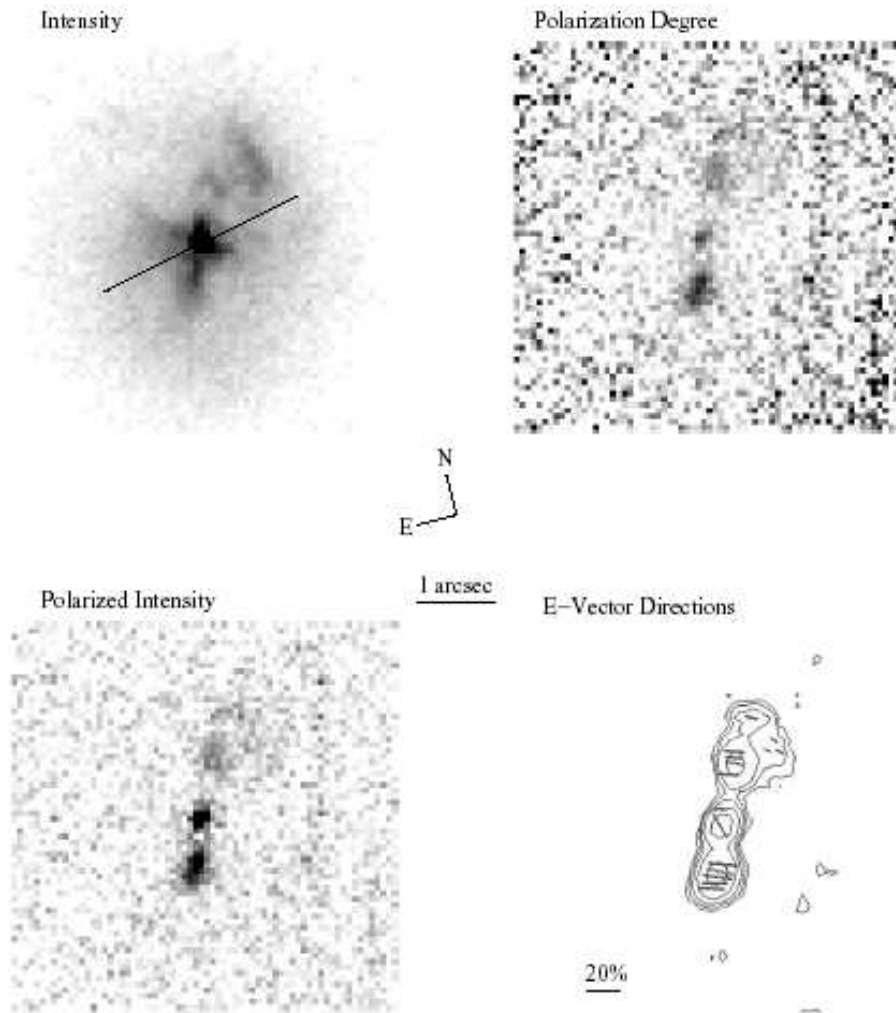


Figure 3. HST/NICMOS  $2.0\mu\text{m}$  intensity and polarization images for the nuclear regions of the powerful radio galaxy Cygnus A (see Tadhunter et al. 2000). The line segment in the intensity image indicates the direction of the radio axis.

## 5. Conclusions

Over the last 20 years optical/IR polarimetry has emerged as a key technique for investigating several aspects of the radio galaxy phenomenon. The diversity of the science made possible by polarimetric studies is impressive, ranging from testing the unified schemes and determining the structure of the near-nuclear regions, to investigating the nature of the host galaxies of some of the most distant known active galaxies.

Polarimetry is likely to remain an important technique in the future, with particular emphasis on using polarimetric observations to probe the sub-kpc structures, quantify the impact of the activity on the host galaxies, and assess the degree of AGN pollution of the host galaxy colours.

Although this review has concentrated on radio galaxies, many of the conclusions also apply to other classes of AGN. For example, the AGN pollution of the host galaxy colours, which is becoming well-quantified for radio galaxies, is likely to be serious (but so far ignored!) issue for the host galaxies of quasars and other types of distant AGN.

## References

- Antonucci, R.J., 1982, *Nat*, 299, 605  
 Antonucci, R.J., 1984, *ApJ*, 278, 499  
 Barthel, P.D., 1989, *ApJ*, 336, 606  
 Brotherton, M.S., Wills, B.J., Dey, A., van Breugel, W., Antonucci, R., 1998, *ApJ*, 501, 110  
 Chambers, K.C., Miley, G.K., Joyce, R.R., 1988, *ApJL*, 329, L75  
 Cimatti, A., di Serego Alighieri, S., Fosbury, R.A.E., Salvati, M., Taylor, D., 1993, *MNRAS*, 264, 421  
 Cimatti, A., di Serego Alighieri, S., 1995, *MNRAS*, 273, L7  
 Cimatti, A., Dey, A., van Breugel, W., Antonucci, R., Spinrad, H., 1996, *ApJ*, 465, 145  
 Cimatti, A., Dey, A., van Breugel, W., Hurt, T., Antonucci, R., 1997, *ApJ*, 476, 677  
 Cimatti, A., di Serego Alighieri, S., Vernet, J., Cohen, M., Fosbury, R.A.E., 1998, *ApJ*, 499, 21  
 Cohen, H.H., Vermeulen, R.C., Ogle, P.M., Tran, H.D., Goodrich, R.W., 1997, *ApJ*, 484, 193  
 Cohen, M.H., Ogle, P.M., Tran, H.D., Goodrich, R.W., Miller, J.S., 1999, *AJ*, 118, 1963  
 Corbett, E.A., Robinson, A., Axon, D.J., Young, S., Hough, J.H., 1998, *MNRAS*, 296, 721  
 Corbett, E.A., Robinson, A., Axon, D.J., Young, S., 2000, *MNRAS*, 319, 685  
 Dey, A., Spinrad, H., 1996, *ApJ*, 459, 133  
 Dey, A., Cimatti, A., van Breugel, W., Antonucci, R., Spinrad, H., 1996, *ApJ*, 465, 157  
 Dey, A., van Breugel, W., Vacca, W.D., Antonucci, R., 1997, *ApJ*, 490, 698  
 di Serego Alighieri, S., Binette, L., Courvoisier, T.J.-L., Fosbury, R.A.E., Tadhunter, C.N., 1988, *Nat*, 341, 307  
 di Serego Alighieri, S., Fosbury, R.A.E., Quinn, P.J., Tadhunter, C.N., 1989, *Nat*, 341, 307  
 di Serego Alighieri, S., Cimatti, A., Fosbury, R.A.E., 1993, *ApJ*, 404, 584  
 di Serego Alighieri, S., Cimatti, A., Fosbury, R.A.E., 1994, *ApJ*, 431, 123  
 di Serego Alighieri, S., Cimatti, A., Fosbury, R.A.E., Hes, R., 1997, *A&A*, 328, 510  
 Draper, P.W., Scarrott, S.M., Tadhunter, C.N., 1993, *MNRAS*, 262, 1029  
 Fabian, A.C., 1989, *MNRAS*, 238, 41p  
 Goodrich, R.W., Cohen, M.H., 1992, *ApJ*, 391, 623  
 Hurt, T., Antonucci, R., Cohen, R., Kinney, A., Krolik, J., 1999, *ApJ*, 514, 579  
 Impey, C.D., Lawrence, C.R., Tapia, S., 1991, *ApJ*, 375, 461  
 Jackson, N., Browne, I.W.A., 1990, *Nat*, 343, 43  
 Jackson, N.J., Tadhunter, C.N., 1993, *A&A*, 272, 105  
 Jackson, N., Tadhunter, C., Sparks, W.B., 1998, *MNRAS*, 301, 131  
 Januzzi, B.T., Elston, R., 1991, *ApJL*, 366, L69  
 Kishimoto, M., Antonucci, R., Cimatti, A., Hurt, T., Dey, A., van Breugel, W., Spinrad, H., 2001, *ApJ*, 547, 667  
 Kishimoto, M., Antonucci, R., Blaes, O., 2003, *MNRAS*, 345, 253

- Lilly, S.J., Longair, M.S., McLean, I.S., 1983, *Nat*, 301, 488  
Lilly, S.J., Longair, M.S., 1984, *MNRAS*, 211, 833  
Manzini, A., di Serego Alighieri, S., 1996, *A&A*, 311, 79  
McCarthy, P.J., van Breugel, W., Spinrad, H., Djorgovski, S., 1987, *ApJL*, 321, 321, L29  
Ogle, P.M., Cohen, M.H., Miller, J.S., Tran, H.D., Fosbury, R.A.E., Goodrich, R.W., 1997, *ApJ*, 482, L370  
Pringle, J., 1997, *MNRAS*, 292, 136  
Scarrott, S.M., Rolph, C.D., Tadhunter, C.N., 1990, *MNRAS*, 243, p5  
Shaw, M., Tadhunter, C., Dickson, R., Morganti, R., 1995, *MNRAS*, 275, 703  
Simpson, C., Ward, M.J., Wilson, A.S., 1995, *ApJ*, 454, 683  
Smith, J.E., Robinson, A., Alexander, D.M., Young, S., Axon, A.J., Corbett, E.A., 2004, *MNRAS*, 350, 140  
Tadhunter, C.N., Scarrott, S.M., Rolph, C.D., 1990, *MNRAS*, 246, 163  
Tadhunter, C.N., Fosbury R.A.E., di Serego Alighieri, S., 1988. In: *BL Lac Objects: Proceedings of the Como Conference 1988*, p79, eds Maraschi, Maccacaro, Ulrich, Springer-Verlag.  
Tadhunter, C., Scarrott, S., Draper, P., Rolph, C., 1992, *MNRAS*, 256, 53p  
Tadhunter, C.N., Shaw, M.A., Morganti, R., 1994, *MNRAS*, 271, 807  
Tadhunter, C., Dickson, R., Shaw, M., 1996, *MNRAS*, 281, 591  
Tadhunter, C.N., Packham, C., Axon, D.J., Jackson, N.J., Hough, J.H., Robinson, A., Young, S., Sparks, W., 1999, *ApJL*, 512, L91  
Tadhunter, C., Sparks, W., Axon D., Bergeron, L., Jackson, N., Packham, C., Hough, J., Robinson, A., Young, S., 2000, *MNRAS*, 313, L52  
Tadhunter, C., Dickson, R., Morganti, R., Robinson, T.G., Wills, K., Villar-Martin, M., Hughes, M., 2002, *MNRAS*, 300 977  
Tadhunter, C., Marconi, A., Axon, D., Wills, K., Robinson, T.G., Jackson, N., 2003, *MNRAS*, 342, 995  
Tran, H.D., Cohen, M.H., Goodrich, R.W., 1995, *AJ*, 110, 2597  
Tran, H.D., Cohen, M.H., Ogle, P.M., Goodrich, R.W., di Serego Alighieri, S., 1998, *ApJ*, 500, 660  
van Bemmell, I.M., Vernet, J., Fosbury, R.A.E., Lamers, H., 2003, *MNRAS*, 345, L13  
Vernet, J., Fosbury, R.A.E., Villar-Martin, M., Cohen, M.H., Cimatti, A., di Serego Alighieri, S., Goodrich, R.W., 2001, *A&A*, 370, 407

### Appendix I: Optical/UV polarization studies of radio galaxies

**Table 1.** Compilation of references for optical/UV polarimetry observations of radio galaxies. The first column gives the references in chronological order. The second column gives the type of polarimetry observation (Key: Sp – spectropolarimetry; Im – imaging polarimetry (with polarization map); Ap – aperture polarimetry at single wavelength; Ap(Im) – aperture polarimetry measurement derived from imaging polarimetry data). The third column gives the number of objects included in the study. The final column gives the redshift range covered by the study.

Reference	Type of study	Number of objects	Redshift range
Antonucci (1982)	Sp	10	$z < 0.256$
Antonucci (1984)	Sp	31	$z < 0.256$
di Serego Alighieri et al. (1988)	Ap(Im)	1(PKS2152-69)	$z = 0.0283$
di Serego Alighieri et al. (1989)	Ap(Im)	2	$z = 0.766$ & $1.132$
Tadhunter et al. (1990)	Im	1(Cygnus A)	$z = 0.0560$
Scarrott et al. (1990)	Im	1(3C368)	$1.132$
Januzzi & Elston (1991)	Ap(Im)	1(3C265)	$z = 0.81$
Impey et al. (1991)	Ap	20	$z < 0.549$
Goodrich & Cohen (1992)	Sp	1(3C109)	$z = 0.3066$
Tadhunter et al. (1992)	Ap(Im)	12	$0.2 < z < 0.85$
Jackson & Tadhunter (1993)	Sp	1(Cygnus A)	$z = 0.056$
di Serego Alighieri et al. (1993)	Ap(Im)	6	$0.380 < z < 1.206$
Draper et al. (1993)	Im	4	$0.041 < z < 0.22$
Cimatti et al. (1993)	Ap(Im),Sp	42	$0.096 < z < 1.206$
di Serego Alighieri et al. (1994)	Sp	3	$0.766 < z < 0.818$
Tadhunter et al. (1994)	Ap(Im)	1(PKS1934-63)	$z = 0.183$
Cimatti & di Serego Alighieri (1995)	Im,Ap(Im)	8	$0.096 < z < 1.206$
Shaw et al. (1995)	Im(Ap)	4	$0.3 < z < 0.7$
Tran et al. Cohen (1995)	Sp	1(3C234)	$z = 0.1848$
Dey & Spinrad (1996)	Sp	1(3C265)	$z = 0.81$
Cimatti et al. (1996)	Sp	1(3C324)	$z = 1.2$
Dey et al. (1996)	Sp	1(3C256)	$z = 1.824$
Tadhunter et al. (1996)	Sp	1(3C321)	$z = 0.096$
Cimatti et al. (1997)	Sp	2	$z = 1.08$ & $1.35$
di Serego Alighieri et al. (1997)	Sp	9	$0.086 < z < 0.258$
Ogle et al. (1997)	Sp,Im	1(Cygnus A)	$z = 0.056$
Cohen et al. (1997)	Sp,Im,Ap	1(PKS0116+082)	$z = 0.594$
Dey et al. (1997)	Sp	1(4C41.17)	$z = 3.8$
Cimatti et al. (1998)	Sp	2	$z = 2.482$ & $2.366$
Tran et al. (1998)	Sp,Im	4	$0.75 < z < 1.2$
Corbett et al. (1998)	Sp	5	$0.057 < z < 0.286$
Brotherton et al. (1998)	Sp	1(3C68.1)	$z = 1.228$
Hurt et al. (1999)	Im(UV)	8	$0.056 < z < 0.58$
Cohen et al. (1999)	Sp,Im	13	$0.056 < z < 0.185$
Corbett et al. (2000)	Sp	4	$0.057 < z < 0.371$
Vernet et al. (2001)	Sp	9	$2.26 < z < 3.56$
Kishimoto et al. (2001)	Sp,Im(UV)	3	$0.096 < z < 0.185$
Tadhunter et al. (2002)	Ap(Im)	19	$0.15 < z < 0.7$
van Bemmell et al. (2003)	Sp	1(Cygnus A)	$z = 0.056$